Electronic Supplementary Material (ESI) for Journal of Materials Chemistry C.

Antisolvent Polysulfone Dielectric for Ultrastable Solution-Processed High-Performance Conformal Organic Transistor Array

Mingxin Zhang,† Mengqiao Du,† Yanhong Tong,* Xue Wang, Jing Sun, Shanlei Guo, Xiaoli Zhao, Qingxin Tang, * and Yichun Liu

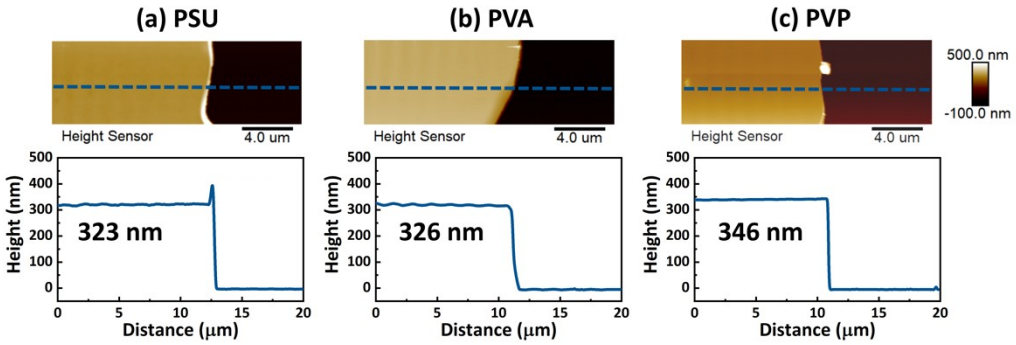

Fig. S1. The thickness of PSU, PVA, and PVP film.

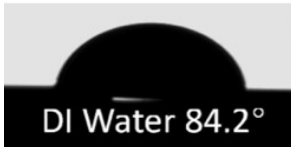

Fig. S2. The contact angle of PSU dielectric.

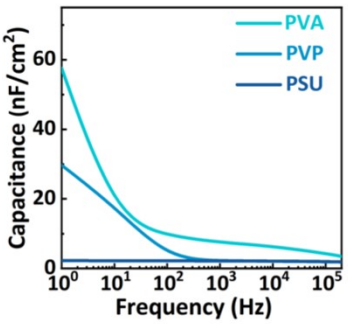

Fig. S3. The capacitance-frequency curves of PVA, PVP, and PSU dielectrics.

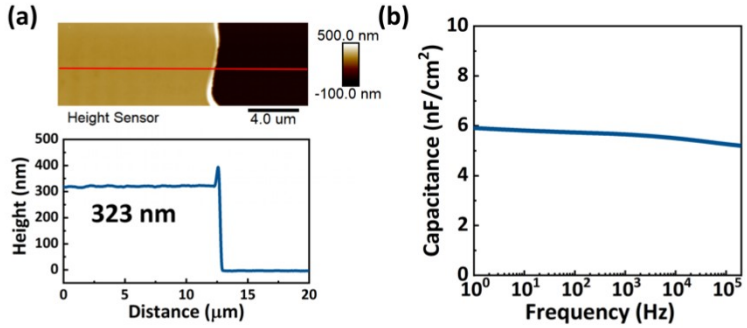

Fig. S4. (a) AFM images of the dielectric thickness and (b) capacitance-frequency curves of PSU dielectric.

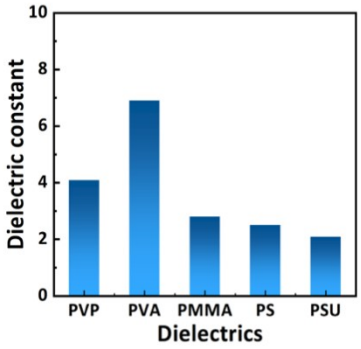

Fig. S5. The dielectric constant of PVA, PVP, PMMA, PS, and PSU.

Table S1. The transmittance of the reported OFETs.

Semiconductor	Electrode	Gate electrode	Dielectric	Transmittance（%）	Ref.
IGZO	ITO	ITO	Al_2O_3	＞60 %	[1]
In_2O_3	Graphene/Au	Graphene/Au	ZAO	90 %	[2]
IZO	ITO	ITO	Al_2O_3	80 %	[3]
R-GO/PU	(PEDOT:PSS)/PUD	(PEDOT:PSS)/PUD	PU	75 %	[4]
Graphene	Graphene	Graphene	SU-8 epoxy	70 %	[5]
S-SWCNT	AgNW	AgNW/PUA	PU-co-PEO	/	[6]
Graphene	Graphene/AgNW	Graphene/AgNW	parylene	＞80 %	[7]
SWCNT	(AgNW)-PUA	(AgNW)-PUA	PU-co-PEG	＞90 %	[8]
CNT	Graphene	Graphene	Al_2O_3	80 %	[9]
Graphene	Graphene	PEDOT:PSS	ion gel	/	[10]
C8-BTBT	PEDOT:PSS /SWCNT	PEDOT:PSS /SWCNT	c-PVA	＞80 %	[11]
C8-BTBT	Au	Au	c-PVA	>80 %	[12]
29-DPP-TVT	PEDOT:PSS	PEDOT:PSS	PVF	>80 %	[13]
C8-BTBT/PS	Ag	ITO	PVP-HDA	>90 %	[14]
C8-BTBT	Au	PEDOT：PSS	PSU	96.1 %	Our work

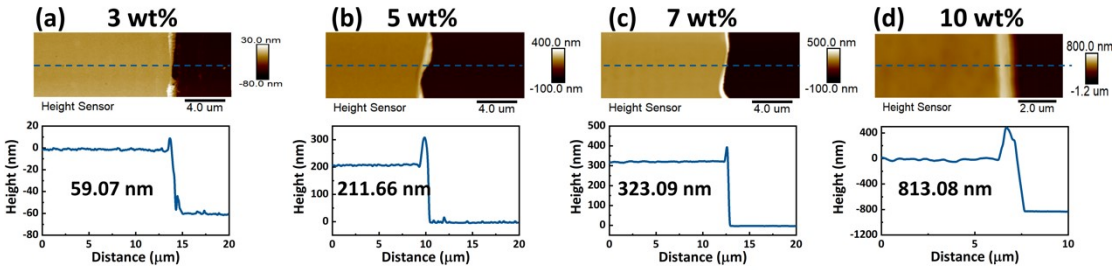

Fig. S6. The AFM images and dielectric thickness of the different PSU thickness OFETs.

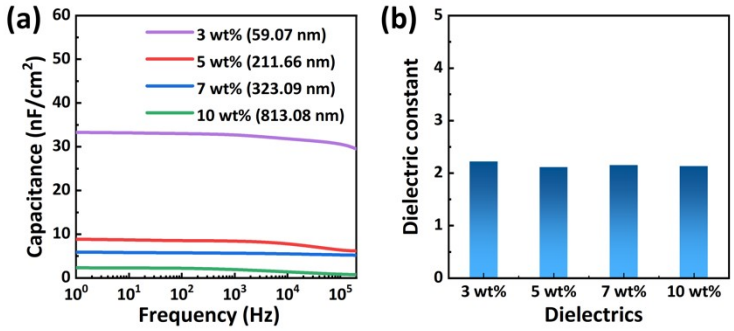

Fig. S7. The capacitance and dielectric constant of PSU dielectric.

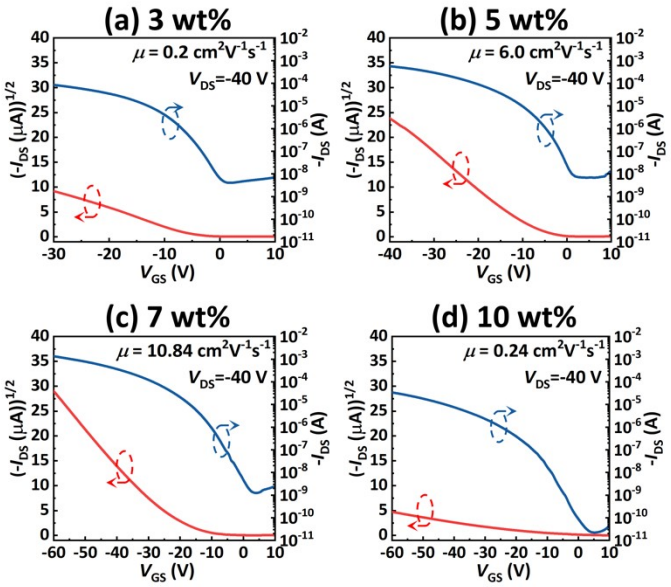

Fig. S8. The transfer curves of different thickness of PSU dielectric OFETs.

Table S2. Parameters for the PSU dielectric OFETs with different dielectric thickness.

Thickness (nm)	**Capacitance (nF/cm^2)**	**Dielectric constant**	**On-state current (A)**	**Mobility ($cm^2V^{-1}s^{-1}$)**
59.07	33.28	2.22	7.94×10^{-5}	0.2
211.66	8.85	2.11	5.56×10^{-4}	6.0
323.09	5.91	2.15	1.29×10^{-3}	10.84
813.08	2.32	2.13	3.28×10^{-5}	0.24

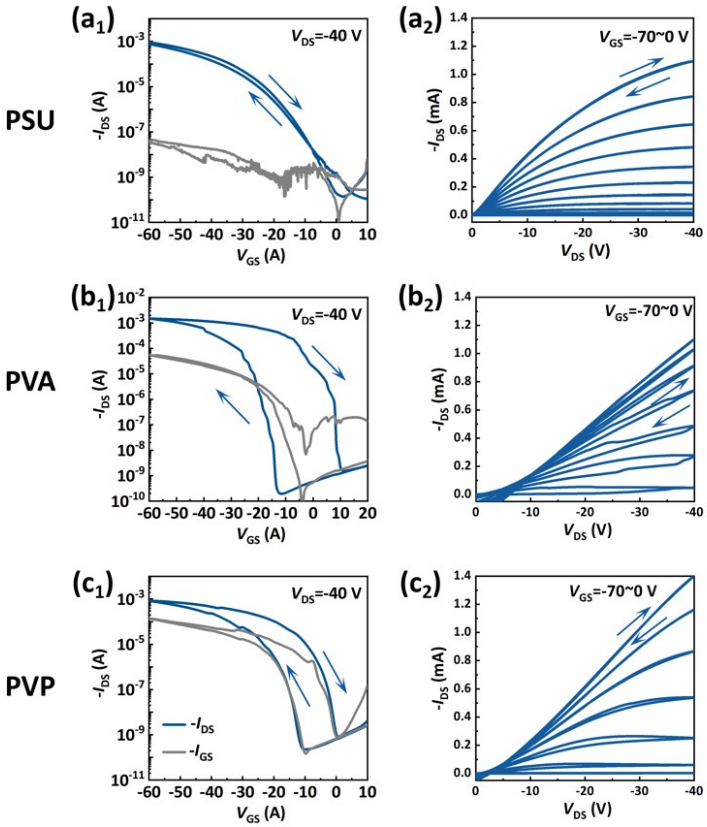

Fig. S9. The double sweep transfer and output curves of PSU, PVA, and PVP dielectric OFET.

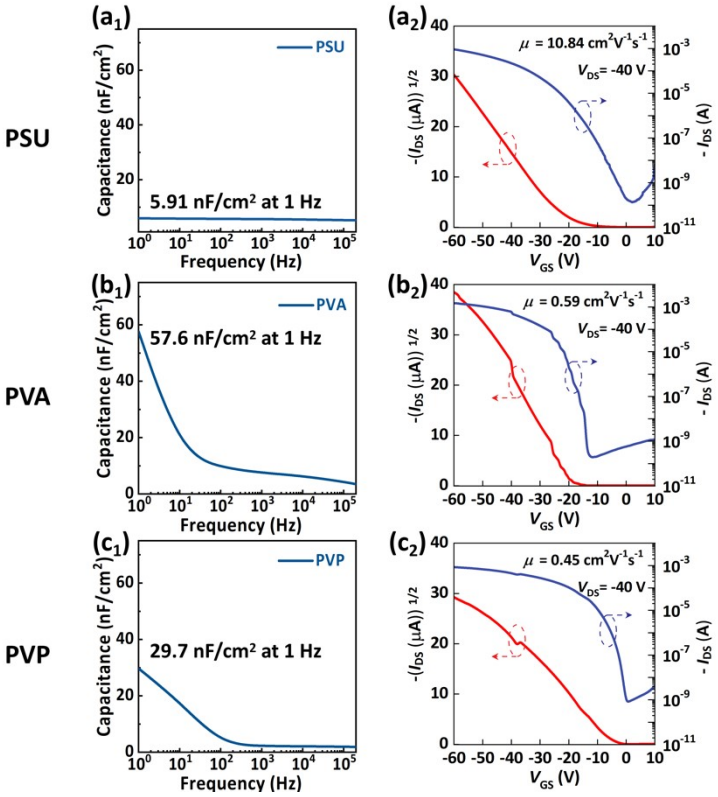

Fig. S10. The capacitance and transfer curves of PSU (a), PVA (b), and PVP (c) dielectric OFETs.

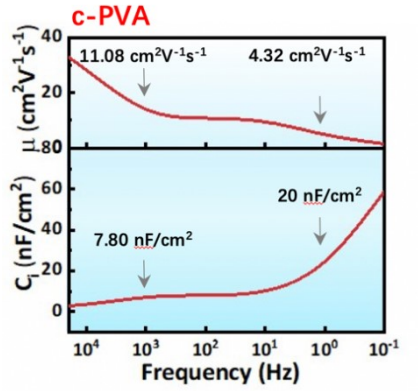

Fig. S11. The capacitance-frequency curves and the calculated mobility at different frequency of c-PVA dielectric OFETs.

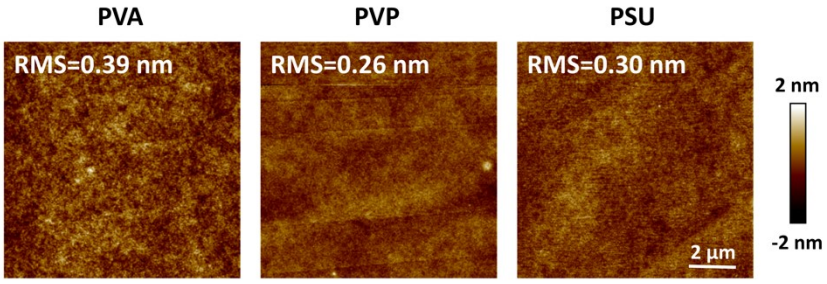

Fig. S12. The surface roughness of PVA, PVP, and PSU dielectrics.

Table S3. The surface energy of PVA, PVP, PSU dielectrics.

Dielectrics	Contact angles		γ^p	γ^d	γ^{total}
	DI water	CH_2I_2	(mJ m^{-2})	(mJ m^{-2})	(mJ m^{-2})
PVA	51	45	18.72	37.01	55.74
PVP	77.36	28.32	3.35	44.90	48.25
PSU	84.2	25	1.37	46.15	47.52
C8-BTBT	91.4	24.5	0.27	46.33	46.60

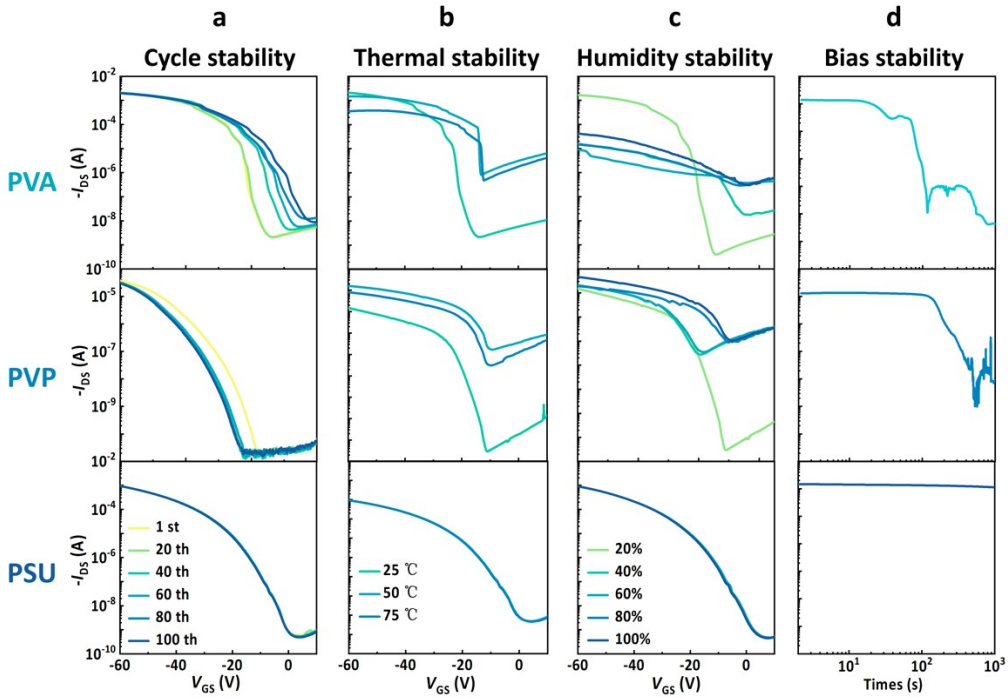

Fig. S13. Highly stable OFETs based on PSU dielectric compared with commercial PVA and PVP dielectrics. (a) Transfer curves within 100 cycles. (b-c) Transfer curves from 25 °C to 75 °C and humidity from 20% to 100%. (d) On-state currents with continuous testing for 1000 s.

Table S4. The polymer dielectric OFETs of the highest humidity.

Dielectrics	**Semiconductor**	**Electrode**	**Humidity (%)**	**Mobility ($cm^2V^{-1}s^{-1}$)**	**Ref.**
PS	Pentacene	Au	40~50%	0.41	[15]
Honey	P3HT	Au	50%	/	[16]
c-dextran	C8-BTBT	Au	20~60%	7.72	[17]
PMMA/PVA	CuPc	Cu	0~100%	0.035	[18]
PMMA/PMMA /PVA/PS/PVP	CuPc	Cu	0~100%	0.015	[19]
PSU	**C8-BTBT**	**Au**	**20~100%**	**10.84**	**Our work**

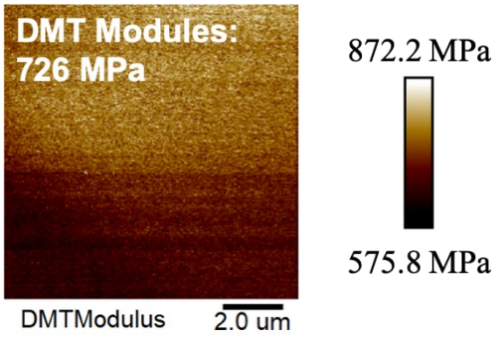

Fig. S14. Young's modules of PSU dielectric.

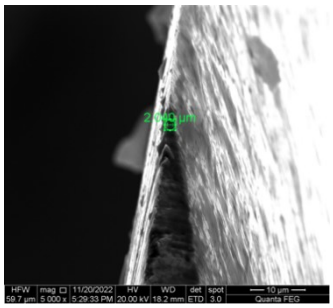

Fig. S15. The SEM images of the1 um bending radius.

References

[1] Wei H, Liu X, Wang A, et al. FeOx-supported platinum singleatom and pseudosingle-atom catalysts for chemoselective hydrogenation of functionalized nitroarenes[J]. Nature Communications, 2014, 5(1): 1-8.

[2] Minari T, Nemoto T, Isoda S. Temperature and electric-field dependence of the mobility of a single-grain pentacene field-effect transistor[J]. Journal of Applied Physics, 2006, 99(3): 034506.

[3] Lee H E, Kim S, Ko J, et al. Skin-like oxide thin-film transistors for transparent displays[J]. Advanced Functional Materials, 2016, 26(34): 6170-6178.

[4] Trung T Q, Ramasundaram S, Hwang B U, et al. An all-elastomeric transparentand stretchable temperature sensor for body-attachable wearable electronics[J]. Advanced Materials, 2016, 28(3): 502-509.

[5] Park Y J, Lee S K, Kim M S, et al. Graphene-based conformal devices[J]. ACS Nano, 2014, 8(8): 7655-7662.

[6] Liang J, Tong K, Pei Q. A water-based silver-nanowire screen-print ink for the fabrication of stretchable conductors and wearable thin-film transistors[J]. Advanced Materials, 2016, 28(28): 5986-5996.

[7] Kim J, Lee M S, Jeon S, et al. Highly transparent and stretchable field-effect transistor sensors using graphene-nanowire hybrid nanostructures[J]. Advanced Materials, 2015, 27(21): 3292-3297.

[8] Liu J, Zhang H, Dong H, et al. High mobility emissive organic semiconductor[J]. Nature Communications, 2015, 6(1): 10032.

[9] Chae S H, Yu W J, Bae J J, et al. Transferred wrinkled Al_2O_3 for highly stretchable and transparent graphene-carbon nanotube transistors[J]. Nature Materials, 2013, 12(5): 403-409.

[10] Lee S K, Kim B J, Jang H, et al. Stretchable graphene transistors with printed dielectrics and gate electrodes[J]. Nano Letters, 2011, 11(11): 4642-4646.

[11] Cui N, Tang Q, Ren H, et al. A photolithographic stretchable transparent electrode for an all-solution-processed fully transparent conformal organic transistor array[J]. Journal of Materials Chemistry C, 2019, 7(18): 5385-5393.

[12] Cui N, Ren H, Tang Q, et al. Fully transparent conformal organic thin-film transistor array and its application as LED front driving[J]. Nanoscale, 2018, 10(8): 3613-3620.

[13] Viola F A, Barsotti J, Melloni F, et al. A sub-150-nanometre-thick and ultraconformable solution-processed all-organic transistor[J]. Nature Communications, 2021, 12(1): 5842.

[14] Yuan Y, Giri G, Ayzner A L, et al. Ultra-high mobility transparent organic thin film transistors grown by an off-centre spin-coating method[J]. Nature Communications, 2014, 5(1): 3005.

[15] Nigam A, Kabra D, Garg T, et al. Insight into the charge transport and degradation mechanisms in organic transistors operating at elevated temperatures in air[J]. Organic Electronics, 2015, 22: 202-209.

[16] Sharova A S, Caironi M. Sweet electronics: Honey-gated complementary organic transistors and circuits operating in air[J]. Advanced Materials, 2021, 33(40): 2103183.

[17] Yang Y, Sun H, Zhao X, et al. High-Mobility Fungus-Triggered Biodegradable Ultraflexible Organic Transistors[J]. Advanced Science, 2022, 9(13): 2105125.

[18] Subbarao N V V, Gedda M, Iyer P K, et al. Organic field-effect transistors as high performance humidity sensors with rapid response, recovery time and remarkable ambient stability[J]. Organic Electronics, 2016, 32: 169-178.

[19] Subbarao N V V, Gedda M, Iyer P K, et al. Enhanced environmental stability induced by effective polarization of a polar dielectric layer in a trilayer dielectric system of organic field-effect transistors: a quantitative study[J]. ACS applied materials & interfaces, 2015, 7(3): 1915-1924.